Electron-hole exchange interaction in a negatively charged quantum dot

I. A. Akimov,[1,2] K. V. Kavokin,[2] A. Hundt,[1] and F. Henneberger[1,*]
[1]*Humboldt Universität zu Berlin, Institut für Physik, Newtonstrasse 15, 12489 Berlin, Germany*
[2]*A.F. Ioffe Physical-Technical Institute, Polytekhnicheskaya 26, 194021 St. Petersburg, Russia*
(Received 16 July 2004; revised manuscript received 20 October 2004; published 25 February 2005)

The fine structure of the "excited-electron" trion triplet state in negatively charged CdSe/ZnSe self-assembled quantum dots is studied using polarization-selective as well as magneto-photoluminescence spectroscopy on a single-dot level. The charged biexciton emission where the optically active triplet states with total angular momentum projections $\pm\frac{1}{2}$ and $\pm\frac{3}{2}$ are left behind is used as a monitor. The line separation provides an energy of $\tilde{\Delta}_0 = 1.5$ meV for the isotropic electron-hole exchange interaction. The anisotropic electron-hole exchange creates a mixing between $\pm\frac{1}{2}$ and $\mp\frac{3}{2}$ triplet states resulting in partially linear polarization as well as specific g factors of the optical transitions. Studying experimentally both types of manifestations, we find a ratio between the anisotropic and isotropic part of $\tilde{\Delta}_1/\tilde{\Delta}_0 \approx 0.5$, distinctly larger than for the exciton in uncharged quantum dots. This is caused by the fact that the electron participating in the exchange is in an excited state enhancing the anisotropy.

DOI: 10.1103/PhysRevB.71.075326 PACS number(s): 78.55.Et, 78.67.Hc, 71.35.Pq

I. INTRODUCTION

The discrete energy spectrum of semiconductor quantum dots (QDs), apart from making them attractive for various device applications, offers diversified and often unexpected opportunities for studying the basic principles of quantum mechanics experimentally. However, though they are often called "artificial atoms," the semiconductor nature of QDs produces characteristic peculiarities that manifest in novel electronic and optical properties. For example, optical excitation of an electron from a valence-band to a conduction-band level is equivalent to the formation of an electron-hole pair. The exchange interaction between electron and hole lifts the degeneracy of the spin states and gives rise to specific fine structures.[1] The ground-state exciton in self-assembled QDs has been widely studied in this regard, both experimentally[2–7] and theoretically.[8,9] The heavy-hole exciton comprises four states with total angular momentum projection $F_z = s_z + j_z$, where $s_z = \pm 1/2$ is the electron spin and $j_z = \pm 3/2$ is the hole angular momentum projection, respectively. The optically allowed states with $F_z = \pm 1$ are separated from the nonradiative states with $F_z = \pm 2$ by the isotropic electron-hole exchange (EHX) with an energy Δ_0. In the presence of in-plane anisotropy, the so-called long-range EHX further splits the radiative doublet into two lines with linear polarizations along the principal axes of the QD. This energy splitting Δ_1 is typically one order of magnitude smaller than Δ_0. In general, the nonradiative doublet is also split by an energy Δ_2, but magnetic-field data demonstrate that Δ_2 is within the optical linewidth.[4]

Charged excitons or trions as the fundamental optical excitations of charged QDs have recently attracted growing interest.[10–20] The presence of a resident carrier changes the total spin of the system from integer to half integer. As a result, the fine structure of the energy spectrum as well as the polarization properties of the optical transitions transform profoundly. According to the Kramers theorem, the eigenstates of the trion are doublets degenerate in the absence of a magnetic field, regardless of the QD symmetry. In the case of a negative resident charge investigated throughout this paper, the trion ground-state consists of two electrons with antiparallel spins in the lowest electron shell ($1e$) and one hole in the lowest hole shell ($1h$). Since the total electron spin S is zero, there is no EHX interaction and, as a consequence, a single resonance appears in the optical spectra. This is no longer true when one of the electrons is promoted to a higher energy shell. Such an "excited-electron" trion is an interesting object as it provides rich information on the EHX interactions in QDs.[21]

There is a hierarchy of energy scales. The exchange interaction between two identical particles is much stronger than the one between electron and hole. The electron-electron exchange interaction, with typical energies in the 10-meV range, splits the excited-electron trion into a singlet state with $S=0$, $S_z=0$ and, situated at lower energies, a triplet state with $S=1$, $S_z=0,\pm 1$, all degenerate with respect to the hole angular momentum $j_z = \pm 3/2$. Δ_0 is on a 1-meV energy scale and the EHX can be hence considered as an interaction of the hole angular momentum $\boldsymbol{j}$ with the total spin of the electrons $\boldsymbol{S} = \boldsymbol{s_1} + \boldsymbol{s_2}$. It splits the otherwise sixfold degenerate triplet state into a set of three doublets with $F_z = \pm 1/2, \pm 3/2, \pm 5/2$, where $F_z = S_z + j_z$. As those Kramers doublets cannot be split further without a magnetic field, the Hamiltonian describing the EHX interaction for a trion in the triplet state can be written in the reference frame of the principal QD axes as

$$H_{\mathrm{EHX}} = \begin{pmatrix} \tilde{\Delta}_0 & \frac{\tilde{\Delta}_1}{\sqrt{2}} & 0 \\ \frac{\tilde{\Delta}_1}{\sqrt{2}} & 0 & \frac{\tilde{\Delta}_2}{\sqrt{2}} \\ 0 & \frac{\tilde{\Delta}_2}{\sqrt{2}} & -\tilde{\Delta}_0 \end{pmatrix}, \qquad (1)$$

where rows and columns are numerated in incremental order of $|F_z|$ and $\tilde{\Delta}_i = (\Delta_i^1 + \Delta_i^2)/2$ with superscript numbers 1 and 2

denoting the exchange energy of the first and second electron, respectively, with the trion hole.[21] Note that these energies are different as the electrons belong to different orbital wave functions. The diagonal part of H_{EHX} is responsible for the energy splitting between the doublets, while the nondiagonal elements provide a mixing of pure F_z states. In the exciton, Δ_1 couples states with $\Delta F_z = \pm 2$ and Δ_2 those with $\Delta F_z = \pm 4$. This translates into a coupling of $|\pm\frac{3}{2}\rangle$ and $|\mp\frac{1}{2}\rangle$ as well as of $|\pm\frac{3}{2}\rangle$ and $|\mp\frac{5}{2}\rangle$ in the trion triplet state. As we shall see below, the mutual admixture of states with different total angular momentum caused by in-plane anisotropy drastically modifies the polarization and magnetic properties of the optical transitions in a charged QD.

Recently, the above fine structure of the "excited-electron" trion has been indeed revealed in various studies, both on a single-dot level[19,22–24] as well as by time- and polarization-resolved photoluminescence (PL) spectroscopy on QD ensembles.[25] Moreover, the triplet state has been invoked as a source for the realization of optically driven spin devices using charged QDs.[26] Knowledge of the energy structure and the polarization properties of the trion triplet state is thus of both fundamental and practical interest. However, no detailed comparison between experiment and theory has been carried out so far and many questions are still open. For example the strength of the anisotropic EHX part $\tilde{\Delta}_1$, as a critical issue in the context of spin control, has not yet been elaborated.

In this work, we present a comprehensive study of the spin-related fine structure of the trion triplet state in self-assembled CdSe/ZnSe QD structures. Use of II-VI QDs, where the typical EHX energies are at least an order of magnitude larger than for III-V materials, has the advantage that the fine structure can be directly resolved in the spectral domain. We apply polarization-selective PL as well as magneto-PL spectroscopy on a single-dot level, since the characteristic features will be otherwise hidden by the inhomogeneous broadening. The PL signal from the triplet state itself can be hardly used for our purpose, as its lifetime is determined by the relaxation in the trion ground-state.[19] Extending previous work,[19,22,23] our experimental concept relies on the PL from the negatively charged biexciton where the triplet state is left behind as the final state of the radiative recombination. The paper is organized as follows. In Sec. II, we describe the samples investigated, the experimental setup as well as the spectral features on which the further analysis is based. In Sec. III, the polarization properties of the PL from trions and charged biexcitons are discussed. In Sec. IV, we present magneto-optical data and extract the longitudinal g factors from the Zeeman splittings (Faraday geometry). Each of the measurements—polarization and Zeeman splitting—allows us to determine separately the ratio between the anisotropic and isotropic EHX. Surprisingly, both methods yield that $\tilde{\Delta}_1$ and $\tilde{\Delta}_0$ are of the same order of magnitude.

II. EXPERIMENTAL AND PHOTOLUMINESCENCE STRUCTURE OF NEGATIVELY CHARGED QUANTUM DOTS

The CdSe/ZnSe QD structures were grown by molecular beam epitaxy using a thermal activation procedure.[27] The QDs with an area density of 10^{11} cm^{-2} are situated on top of a 2 monolayer thick CdSe wetting layer and are embedded between ZnSe buffers. Height and radius of the pure CdSe core are about 2 nm and 5–10 nm, respectively, as revealed by transmission electron microscopy.[28] ZnSe, as many other II-VI compounds, is naturally n type.[29] Therefore, though the samples were not intentionally doped, a certain amount of QDs have captured donor electrons from the surrounding ZnSe.

Electron-hole pairs were excited nonresonantly with the 488 nm Ar^+ laser line ($\hbar\omega_{\mathrm{exc}} = 2.54$ eV) above the wetting-layer continuum edge.[30] The samples were mounted either in a helium flow micro-PL cryostat or in a split-coil helium cryostat capable of magnetic fields up to 12 T. The PL signal was dispersed in a single-grating monochromator with a linear dispersion of 0.24 nm/mm and detected with a charge-coupled-device (CCD) matrix. The experiments were carried out in backward geometry with the propagation directions of both incident and detected light parallel to the [001] growth direction, coinciding also with the orientation of the magnetic field when applied. In all measurements, the temperature is below 10 K. Polarization control was achieved by means of halfwave plate used both in excitation and detection. The excitation laser was strictly linearly polarized.

The overall PL from the QD ensemble is centered at about 2.4 eV. The band has an inhomogeneous width of about 70 meV caused by size and shape fluctuations. Access to single QDs is accomplished by preparing mesas with lateral dimensions of 100 nm by electron beam lithography and wet chemical etching. Careful inspection shows that some of the single-dot PL features represent indeed emission from QDs charged with a single electron.[19] Figure 1 depicts a typical example for low and moderate excitation intensity P. For $P < 200$ W/cm^2, the spectrum consists of a single line labeled by X^-. The yield of X^- grows linearly with P indicating that a single electron-hole pair excitation is involved. The trionic nature is clearly demonstrated in a transverse magnetic field B where the line splits in four components.[19] As expected, all components merge into a single line when their position is extrapolated to $B=0$. In marked contrast, the exciton emission from uncharged QDs of the same mesa exhibits a zero-field splitting of $\Delta_0 = 1.9$ meV between optically allowed and dark states as well as an anisotropy-related splitting between the radiative states of $\Delta_1 \approx 0.2$ meV in average.[4,31] PL excitation measurements have yielded that the excited-electron triplet state is high-energy shifted by about 80 meV.[23,32]

At higher excitation levels, additional lines appear [see Fig. 1(b)]. The weak line close to X^- grows sublinear as a function of P. In other QDs, even more lines of this kind are found, however, with considerable scatter in their energy positions, even occurring on the high-energy side of X^-. Moreover, their yield is substantially reduced when the excitation energy is below the wetting-layer continuum edge. We attribute these lines to recombination of the trion perturbed by defects in the vicinity of the QD, randomly charged by photoexcited carriers.[33] In the rest of this paper, we ignore these lines and concentrate on the doublet feature labeled by XX_1^- and XX_2^-. Systematically, on all QDs studied, this doublet is present 6–10 meV energetically below the trion peak with a

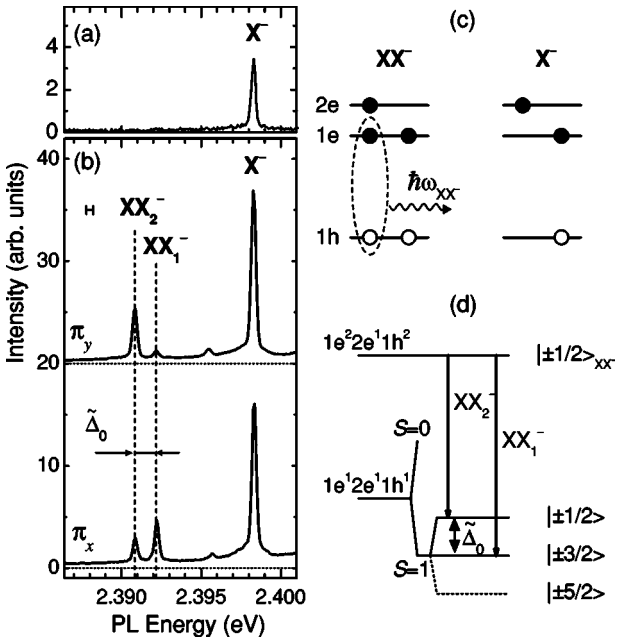

FIG. 1. PL features of a single negatively charged CdSe QD. (a) Low excitation ($P=100$ W/cm^2): trion ground-state emission. (b) Higher excitation ($P=500$ W/cm^2): Emergence of the charged biexciton lines. π_x and π_y refer to linear polarization detection along [110] and [1$\bar{1}$0], respectively. (c) Illustration of the charged biexction recombination leaving a trion with an excited electron in the final state. (d) Fine structure of the charged biexciton PL. np^N symbolizes that the nth single electron ($p=e$) or hole ($p=h$) energy level is occupied by N particles. The spin wave function is represented by $|F_z\rangle$.

line separation of about 1.5 meV. Several findings demonstrate that XX_1^- and XX_2^- are due to recombination of a charged biexciton.[19,22,23] First, the yield of both lines is a quadratic function of the excitation power, indicative of a two electron-hole pair excitation. Second, time-resolved PL measurements reveal a transition cascade of X^- and $XX_{1/2}^-$ with the biexciton doublet emitted first. Third, as confirmed by two-beam PL excitation spectroscopy, both X^- and $XX_{1/2}^-$ originate from the same QD. As already noted above, the electron-electron exchange for QDs of this size is in the some 10-meV range so that singlet-triplet splitting cannot be responsible for XX_1^- and XX_2^-.

The charged biexciton is formed when two electron-hole pairs, initially created in the energy continuum of the structure, are captured by a charged QD. This five-particle complex consists of two holes and three electrons, as schematically shown in the energy level diagram on the left-hand side of Fig. 1(c). According to the Pauli principle, the angular momenta of the holes as well as the spins of the two electrons in the 1e shell are compensated. The charged biexciton ground-state is hence twice degenerate with respect to the total angular momentum projection $\pm\frac{1}{2}$ defined by the spin of the third electron occupying the second shell. Generally, optical transitions involving electrons and holes from different energy shells have low probability. Therefore, an excited-electron trion is left behind in the charged biexciton recombination as schematized in Fig. 1(c). The part of the properly

TABLE I. Angular momentum selection rules for the charged-biexciton–excited-electron trion triplet transition (photon wave vector parallel to z-direction), $\sigma^{\pm}$ is the respective circular photon polarization, and the prefactor denotes that the transition probability is reduced by 1/2.

	$+\frac{1}{2}$	$+\frac{3}{2}$	$+\frac{5}{2}$	$-\frac{5}{2}$	$-\frac{3}{2}$	$-\frac{1}{2}$
$+\frac{1}{2}$		$1/2\sigma^-$				σ^+
$-\frac{1}{2}$	σ^-				$1/2\sigma^+$	

symmetrized charged biexciton wave function relevant for this process can be written as

$$\left|\pm\frac{1}{2}\right\rangle \propto \left|\pm\frac{1}{2}\right\rangle_{e_2}\left(\left|\frac{1}{2}\right\rangle_e\left|-\frac{1}{2}\right\rangle_{e_1} - \left|-\frac{1}{2}\right\rangle_e\left|\frac{1}{2}\right\rangle_{e_1}\right) \times\left(\left|\frac{3}{2}\right\rangle_h\left|-\frac{3}{2}\right\rangle_{h_1} - \left|-\frac{3}{2}\right\rangle_h\left|\frac{3}{2}\right\rangle_{h_1}\right), \quad (2)$$

where e and h denote the recombining electron-hole pair, while e_1, e_2, and h_1 refer to the electrons and the hole of the trion final state. The set of final states reads

$$\left|\pm\frac{1}{2}\right\rangle = \left|\mp\frac{1}{2}\right\rangle_{e_1}\left|\mp\frac{1}{2}\right\rangle_{e_2}\left|\pm\frac{3}{2}\right\rangle_{h_1},$$

$$\left|\pm\frac{3}{2}\right\rangle = \frac{1}{\sqrt{2}}\left(\left|\frac{1}{2}\right\rangle_{e_1}\left|-\frac{1}{2}\right\rangle_{e_2} + \left|-\frac{1}{2}\right\rangle_{e_1}\left|\frac{1}{2}\right\rangle_{e_2}\right)\left|\pm\frac{3}{2}\right\rangle_{h_1},$$

$$\left|\pm\frac{5}{2}\right\rangle = \left|\pm\frac{1}{2}\right\rangle_{e_1}\left|\pm\frac{1}{2}\right\rangle_{e_2}\left|\pm\frac{3}{2}\right\rangle_{h_1}. \quad (3)$$

Comparison of Eqs. (2) and (3) provides the polarization selection rules listed in Table I. Note that analogous rules apply for the optical transitions of the triplet states themselves, except that the photon occurs here together with the $|\pm\frac{1}{2}\rangle$ final-state electron and its polarization is thus reversed. As the $|\pm\frac{5}{2}\rangle$ states are dark, a doublet is expected for the charged biexciton PL [Fig. 1(d)], as indeed observed experimentally. The line separation is close to the energy $\Delta_0 = 1.9$ meV found for the exciton in uncharged CdSe/ZnSe QDs.[4] In what follows we elaborate more information on the EHX in charged QDs, emphasizing on the role of anisotropic part.

III. POLARIZATION PROPERTIES

In the absence of in-plane anisotropy, that is for D_{2d} symmetry, Δ_1 is zero and the only off-diagonal coupling in the triplet Hamiltonian (1) is produced by Δ_2. Δ_2 defines the exchange splitting in the non-radiative exciton doublet $|\pm 2\rangle$. It is caused by relativistic corrections in the conduction band near the Γ point and is hence usually very small.[1] Both experiment[4] and theory[1] yield values of the order of 1 μeV so that Δ_2 can be safely neglected in the present context. In addition to a nonzero value of Δ_1, in-plane anisotropy in-

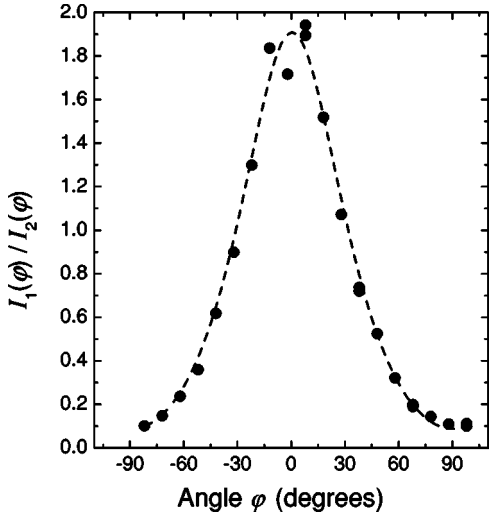

FIG. 2. Ratio of the line intensities of XX_1^- and XX_2^- as a function of the angle between the polarization analyzer and the [110] axis for the same QD as in Fig. 1.

duces also heavy-light hole mixing. For the exciton, both effects can hardly be separated. On the other hand, the trion ground-state is not affected by the EHX so that the pure heavy-light hole coupling can be studied here. Linear built-in polarization and pronounced magnetic anisotropies have been observed.[34] For the present study, we have therefore selected QDs, where the linear polarization degree of the trion ground-state PL is below 0.1, ensuring that the anisotropic EHX is dominant. An additional criterion for the unimportance of heavy-light coupling is the absence of a component related to the $|\pm\frac{5}{2}\rangle$ states in the charged biexciton PL that became allowed otherwise.

The reference frame in the polarization measurements was set with respect to the principal crystal axes as follows: $x\|[110]$, $y\|[1\bar{1}0]$, and $z\|[001]$. In this choice, rotation of the half wave plate allows one to measure the signal intensity in $z(x'y')-z$ configuration in Porto's notation where the angle between x and x' is twice as large as the angle between one of the main axes of the halfwave plate and the x axis. The charged biexciton states $|\pm 1/2\rangle$ are populated with equal probability under the present excitation conditions. For the pure angular momentum triplet states (3), according to Table I, the emission will be totally unpolarized, while already the data in Fig. 1(a) indicate the existence of a preferential polarization axis. The more detailed analysis demonstrates that the polarization directions of XX_1^- and XX_2^- are perpendicular to each other and are related to the [110] and $[1\bar{1}0]$ crystal axes, respectively. In Fig. 2, the angular dependence of the ratio of the line intensities $R(\varphi)=I_1(\varphi)/I_2(\varphi)$ is plotted where φ is defined relative to [110] direction. The accuracy to which $R(\varphi)$ can be measured is better than that of the polarization degree and orientation of each line separately, since I_1 and I_2 can be recorded simultaneously at each angle with the CCD matrix so that adjustment-related deviations in the signal level cancel out. For partly linearly polarized light, the intensity after the analyzer can be expressed through the total intensity I_0 and the maximum degree of linear polarization ρ_L as $I(\varphi)=I_0[1+\rho_L\cos(2\varphi)]$, yielding

$$R(\varphi) = R_0\frac{1+\rho_{L1}\cos(2\varphi)}{1-\rho_{L2}\cos(2\varphi)}, \tag{4}$$

where $R_0=I_{01}/I_{02}$ is the total line ratio and ρ_{L1} and ρ_{L2} are the degrees of linear polarization for XX_1^- and XX_2^-, respectively. A fit to the data provides $R_0=0.55$ as well as $\rho_{L1}=0.74$ and $\rho_{L2}=0.51$.

The ratio R_0 is very close to the theoretical value of $1/2$ in Table I. The finite polarization degree, however, represents direct evidence for the off-diagonal coupling in the EHX Hamiltonian. For $\tilde{\Delta}_2/\tilde{\Delta}_0 \ll 1$, the mixing of $|\pm 5/2\rangle$ and $|\mp 3/2\rangle$ is very small and, as observed experimentally, there is no PL feature related to $|\pm 5/2\rangle$. In this case, the Hamiltonian (1) can be reduced to a 2×2 matrix, the eigenfunctions and energies of which are

$$\phi_1^{\pm} = \cos(\alpha)\left|\pm\frac{3}{2}\right\rangle - \sin(\alpha)\left|\mp\frac{1}{2}\right\rangle,$$

$$\phi_2^{\pm} = \cos(\alpha)\left|\pm\frac{1}{2}\right\rangle + \sin(\alpha)\left|\mp\frac{3}{2}\right\rangle,$$

$$E_1 = \frac{1}{2}(\tilde{\Delta}_0 - \sqrt{(\tilde{\Delta}_0)^2 + 2(\tilde{\Delta}_1)^2}),$$

$$E_2 = \frac{1}{2}(\tilde{\Delta}_0 + \sqrt{(\tilde{\Delta}_0)^2 + 2(\tilde{\Delta}_1)^2}), \tag{5}$$

where $\alpha=\frac{1}{2}\arctan(\sqrt{2}\tilde{\Delta}_1/\tilde{\Delta}_0)$. The optical transitions associated with these states are elliptically polarized, with main axes perpendicular to each other. For the charged biexciton PL, with $\phi_i^{\pm}$ being left behind by XX_i^-, the signal in linear polarization detection has the following parameters:

$$\rho_{L1} = 2\sqrt{2}\frac{\chi}{1+2\chi^2},$$

$$\rho_{L2} = \sqrt{2}\frac{\chi}{1+\frac{1}{2}\chi^2},$$

$$R_0 = \frac{1+2\chi^2}{2+\chi^2} \tag{6}$$

with $\chi=\sqrt{2}\tilde{\Delta}_1/[\tilde{\Delta}_0+\sqrt{\tilde{\Delta}_0^2+2\tilde{\Delta}_1^2}]$. The $1/2$ factor between the transition probabilities of the pure $|\pm\frac{3}{2}\rangle$ and $|\pm\frac{1}{2}\rangle$ states does not only manifest in R_0, but also leads to a larger degree of linear polarization for XX_1^- as compared to XX_2^-. This is in full agreement with the observations shown in Figs. 1(a) and 2. The quantities R_0, ρ_{L1}, and ρ_{L2} are universal functions of the ratio $\tilde{\Delta}_1/\tilde{\Delta}_0$. Their plots in Fig. 3 are compared with the experimental values of R_0, ρ_{L1}, and ρ_{L2} deduced from Fig. 2, yielding a surprisingly large ratio $\tilde{\Delta}_1/\tilde{\Delta}_0\approx 0.55$.

Identical behavior is observed on other negatively charged QDs. In Fig. 4, the energy separation ΔE between X^- and XX_1^-, the energy splitting of XX_1^- and XX_2^-, $\tilde{\Delta}=E_1-E_2$, as well as the ratio between the anisotropic and isotropic part of EHX, $\tilde{\Delta}_1/\tilde{\Delta}_0$, are plotted versus the spectral position of X^-

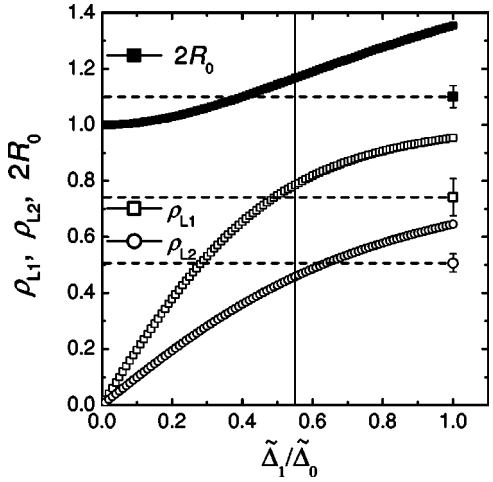

FIG. 3. Intensity ratio R_0 as well as the linear polarization degrees ρ_{1L} and ρ_{2L} versus $\tilde{\Delta}_1/\tilde{\Delta}_0$ according to Eq. (6). The experimental data for the QD in Figs. 1 and 2 are given by the horizontal lines.

for a number of QDs. We find no correlation between these parameters as well as no recognizable dependence on the trion ground-state energy. The lowest scatter occurs for $\Delta E = (7.0 \pm 1.1)$ meV. Unlike the exciton-biexciton energy spacing in neutral QDs, ΔE includes direct and exchange terms of the electron-electron Coulomb interaction involving different shells ($1e$ and $2e$). It can be written as $\Delta E = Q_{X^-} + Q_T - Q_{XX^-}$ where Q_{X^-}, Q_T, and Q_{XX^-} denote the respective few-particle Coulomb energies in the trion ground-state, the first excited (optically allowed) triplet state, and the charged biexciton. The fact that ΔE is positive means that $Q_{XX^-} < Q_{X^-} + Q_T$. Thus, if Q_{X^-} and Q_T are negative, the Coulomb attraction in the biexciton state is stronger than the sum of attraction energies in trion ground-state and the first excited triplet state. The averages of the exchange parameters are $\tilde{\Delta} = (1.5 \pm 0.3)$ meV and $\tilde{\Delta}_1/\tilde{\Delta}_0 = 0.48 \pm 0.14$. From these values, the individual exchange energies summarized in Table II can be deduced as follows: Using $\tilde{\Delta}_0 = (\Delta_0^1 + \Delta_0^2)/2 = \tilde{\Delta}/\sqrt{1+2(\tilde{\Delta}_1/\tilde{\Delta}_0)^2}$ and inserting $\Delta_0^1 = 1.9$ meV and $\Delta_1^1 = 0.2$ meV, previously obtained for the single exciton in uncharged CdSe/ZnSe QDs,[4] i.e., for the $1e$-$1h$ EHX, we find $\Delta_0^2 = 0.6$ meV and $\Delta_1^2 = 0.9$ meV for the $1h$-$2e$ exchange energies. The relation $\Delta_0^2 < \Delta_0^1$ is reasonable as the Coulomb interaction between the $2e$ electron and $1h$ hole is generally weaker as compared to $1h$-$1e$. The same result has been also reported for III-V QDs.[24] On the other hand, the anisotropic part of the $1h$-$2e$ EHX is significantly increased so that Δ_1^2 is even larger than Δ_0^2. The origin of this increase is most likely related to the p-type symmetry of the envelope function of the $2e$ shell enhancing the anisotropy of the EHX.

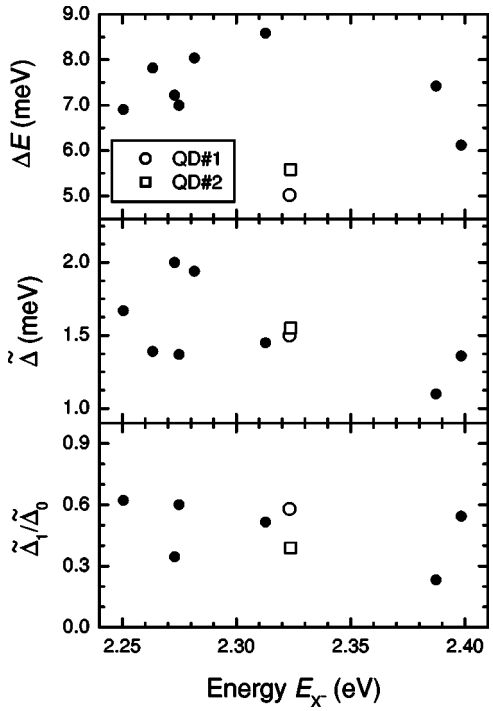

FIG. 4. Energy separation (ΔE) between X^- and XX_1^-, energy splitting ($\tilde{\Delta}$) between the charged biexciton lines XX_1^- and XX_2^- as well as the ratio between the anisotropic and isotropic part of EHX, $\tilde{\Delta}_1/\tilde{\Delta}_0$, plotted versus the spectral position of the X^- PL line for a number of QDs. $\tilde{\Delta}_1/\tilde{\Delta}_0$ is deduced for each QD as demonstrated in Fig. 3. The open symbols mark the QDs studied in magnetic field (see Fig. 5).

TABLE II. Values of isotropic ($i=0$) and anisotropic ($i=1$) EHX energies with superscript numbers 1 and 2 denoting the interaction of the first or second, excited electron, respectively, with the trion hole. The values for Δ_i^1 are from Ref. 4. The total exchange energies in the excited trion state are $\tilde{\Delta}_i = (\Delta_i^1 + \Delta_i^2)/2$.

i	Δ_i^1 (meV)	Δ_i^2 (meV)	$\tilde{\Delta}_i$ (meV)
0	1.9	0.6	1.3
1	0.2	0.9	0.6

IV. ZEEMAN SPLITTING

The impact of the EHX on the trion triplet state is also manifested in the coupling with a longitudinal magnetic field. We have therefore studied the Zeeman splitting of the trion and charged biexciton emission. The experimental data are summarized for two different QDs in Fig. 5. As expected, all three PL features X^-, XX_1^-, and XX_2^- split into doublets. While the X^- emission is strictly circularly polarized with σ^+ (σ^-) rotational direction for the low (high) energy component, the charged biexciton doublets are only preferentially polarized in these directions. The energy difference ΔE^B between the upper and lower components is in a good approximation a linear function of the field strength. This allows us to assign to each PL feature an effective g factor given by $g_L = \Delta E_L^B/\mu_B B$ ($L = X^-, XX_1^-, XX_2^-$), where μ_B is the Bohr magneton. We find that $g_{X^-} = 1.46$ in QD No. 1 as well as $g_{X^-} = 1.52$ in QD No. 2 are indeed close to the exciton g factor of $g_X \approx 1.5$ known from uncharged CdSe/ZnSe QDs.[4,6] On the other hand, $g_{XX_1^-}$ and $g_{XX_2^-}$ are significantly different, both with respect g_{X^-} to as well as relative to each other.

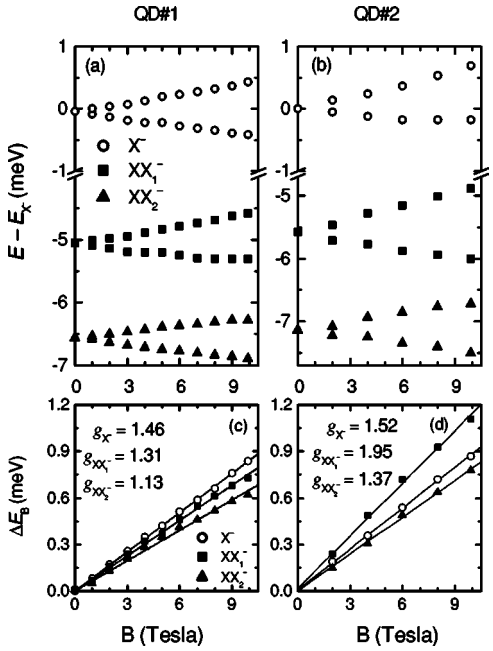

FIG. 5. PL of the trion (X^-) and charged biexciton (XX_1^-, XX_2^-) in a magnetic field applied along the [001] quantization axis for two different QDs. The zero-field data of these QDs are marked in Fig. 4 by open symbols. (a) and (b): Fan charts. (c) and (d): Energy splitting of the Zeeman doublets versus field strength. The g factors deduced from the slopes (see text) are given up left.

The energy diagrams of the trion and charged biexciton recombination in a longitudinal magnetic field are schematically shown in Figs. 6(a) and 6(b), respectively. For the recombination from the trion ground-state, the g factor of the initial state is defined by the hole, while the splitting of the final state is determined by the g factor g_{1e} of the electron left behind in the $1e$ shell. This yields $g_{X^-}=g_h-g_{1e}$ which is indeed equal to the exciton g factor. The g factor of the charged biexciton is given by the g factor g_{2e} of the electron in the $2e$ shell. The g factors associated with the triplet final states are more complex. Let us first ignore the anisotropic EHX ($\tilde{\Delta}_1=0$). Then, as can be easily seen from Eq. (3), $|\pm 1/2\rangle$ has an effective g factor of $g_h-(g_{1e}+g_{2e})$, while that of $|\pm\frac{3}{2}\rangle$ is g_h as for the trion ground-state. Using now the

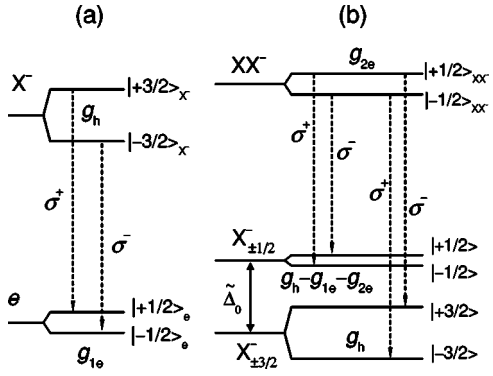

FIG. 6. Transition scheme for the trion (left) and charged biexciton (right) PL in a magnetic field applied along [001] axis.

mixed states $\phi_i^{\pm}$ from Eq. (5), we find in presence of anisotropic EHX

$$g_{XX_1^-}=\frac{g_{1e}-g_{2e}}{2}+\frac{\tilde{\Delta}_0}{\sqrt{(\tilde{\Delta}_0)^2+2(\tilde{\Delta}_1)^2}}\left(g_h-\frac{g_{1e}+g_{2e}}{2}\right),$$

$$g_{XX_2^-}=-\frac{g_{1e}-g_{2e}}{2}+\frac{\tilde{\Delta}_0}{\sqrt{(\tilde{\Delta}_0)^2+2(\tilde{\Delta}_1)^2}}\left(g_h-\frac{g_{1e}+g_{2e}}{2}\right).$$

Interestingly, $g_{XX_1^-}-g_{XX_2^-}$ provides a direct measure of the difference between the electron g factors of the $1e$ and $2e$ shell. In both QDs, we find $g_{XX_1^-}>g_{XX_2^-}$ and hence $g_{e1}>g_{e2}$. The electron g factor in ZnSe ($g_e=1.2$) is three times larger than for CdSe.[35] A stronger penetration of the $1e$ orbital wave function in the ZnSe barrier can thus explain the g factor relation observed experimentally. The $2e$ shell is high-energy shifted by about 80 meV,[22] close to the wetting layer edge. Accordingly, the wave function spreads out into the wetting layer, reducing in parallel its extension in growth direction. This explanation is supported by the fact that fluctuations of $g_{e1}-g_{e2}$ (QD No. 1: 0.2, QD No. 2: 0.6) are more distinct than for $g_{X^-}=g_h-g_{1e}$, indicating that the g factor of the $2e$ shell depends sensitively on the specific confinement conditions in a given QD. The sum of the g factors can be written as

$$g_{XX_1^-}+g_{XX_2^-}=\frac{2g_{X^-}+(g_{XX_1^-}-g_{XX_2^-})}{\sqrt{1+2(\tilde{\Delta}_1/\tilde{\Delta}_0)^2}} \tag{7}$$

and allows us to extract the ratio $\tilde{\Delta}_1/\tilde{\Delta}_0$ in an independent way. We find $\tilde{\Delta}_1/\tilde{\Delta}_0=0.55$ in the QD No. 1 and $\tilde{\Delta}_1/\tilde{\Delta}_0=0.31$ in QD No. 2. Both values are in good agreement with the ratio deduced from the zero-field polarization data. Although the energy of the trion ground-state is almost the same in both QDs, the g factor of the excited electron as well as the exchange parameters are quite different. Therefore, as already mentioned in the previous section, there is no clear relation between the trion ground-state energy and these quantities.

V. CONCLUSIONS

We have studied the electron-hole exchange interaction in negatively charged QDs. The isotropic part gives rise to a specific doublet pattern of the trion triplet state. The isotropic exchange energy agrees well with the one of the exciton in uncharged QDs. To elaborate the anisotropic part, we have selected QDs with almost unpolarized emission from the trion ground-state, ensuring that heavy-light hole coupling is of minor importance. It turns out that the anisotropic exchange interaction is distinctly stronger than for the exciton, though charged and uncharged QDs exhibit the same morphology. We attribute this finding to the fact that the second electron participating in the exchange is in an excited state, for which the orbital wave function has a stronger anisotropy. Our results are also important in the context of optical spin manipulation on charged QDs. The anisotropy-caused mix-

ing enables a combined electron-hole spin flip in the trion triplet state, by which the spin of the resident electron can be aligned.[26] The efficiency of this spin flip is governed by the ratio between anisotropic and isotropic EHX. Therefore, our findings suggest that the large anisotropic part makes the combined spin-flip process indeed an important contribution in the trion relaxation. This point deserves further investigations.

ACKNOWLEDGMENTS

The authors thank S. Rogaschewski for the lithographic etching. Part of this work was supported in the frame of the Center of Excellence 296 funded by the Deutsche Forschungsgemeinschaft. K. K. acknowledges partial support of RFBR and the Russian Academy of Sciences programme "Low-dimensional quantum structures."

*Electronic address: henne@physik.hu-berlin.de

[1] E. L. Ivchenko and G. E. Pikus, *Superlattices and Other Heterostructures: Symmetry and Optical Phenomena* (Springer-Verlag, New York, 1995).
[2] D. Gammon, E. S. Snow, B. V. Shanabrook, D. S. Katzer, and D. Park, Phys. Rev. Lett. **76**, 3005 (1996).
[3] R. I. Dzhioev, B. P. Zakharchenya, E. L. Ivchenko, V. L. Korenev, Yu. G. Kusraev, N. N. Ledentsov, V. M. Ustinov, A. E. Zhukov, and A. F. Tsatsul'nikov, Phys. Solid State **40**, 790 (1998).
[4] J. Puls, M. Rabe, H.-J. Wünsche, and F. Henneberger, Phys. Rev. B **60**, 16 303 (1999).
[5] M. Bayer, A. Kuther, A. Forchel, A. Gorbunov, V. B. Timofeev, F. Schäfer, J. P. Reithmaier, T. L. Reinecke, and S. N. Walck, Phys. Rev. Lett. **82**, 1748 (1999).
[6] V. D. Kulakovskii, G. Bacher, R. Weigand, T. Kümmell, A. Forchel, E. Borovitskaya, K. Leonardi, and D. Hommel, Phys. Rev. Lett. **82**, 1780 (1999).
[7] L. Besombes, K. Kheng, and D. Martrou, Phys. Rev. Lett. **85**, 425 (2000).
[8] S. V. Goupalov, E. L. Ivchenko, and A. V. Kavokin, JETP **86**, 399 (1998).
[9] T. Takagahara, Phys. Rev. B **62**, 16 840 (2000).
[10] R. J. Warburton, C. S. Dürr, K. Karrai, J. P. Kotthaus, G. Medeiros-Ribeiro, and P. M. Petroff, Phys. Rev. Lett. **79**, 5282 (1997).
[11] K. H. Schmidt, G. Medeiros-Ribeiro, and P. M. Petroff, Phys. Rev. B **58**, 3597 (1998).
[12] R. J. Warburton, C. Schäflein, D. Haft, F. Bickel, A. Lorke, K. Karrai, J. M. Garcia, W. Schoenfeld, and P. M. Petroff, Nature (London) **405**, 926 (2000).
[13] J. J. Finley, A. D. Ashmore, A. Lemaître, D. J. Mowbray, M. S. Skolnick, I. E. Itskevich, P. A. Maksym, M. Hopkinson, and T. F. Krauss, Phys. Rev. B **63**, 073307 (2001).
[14] F. Findeis, M. Baier, A. Zrenner, M. Bichler, G. Abstreiter, U. Hohenester, and E. Molinari, Phys. Rev. B **63**, 121309 (2001).
[15] K. F. Karlsson, E. S. Moskalenko, P. O. Holtz, B. Monemar, W. V. Schoenfeld, J. M. Garcia, and P. M. Petroff, Appl. Phys. Lett. **78**, 2952 (2001).
[16] D. V. Regelman, E. Dekel, D. Gershoni, E. Ehrenfreund, A. J. Williamson, J. Shumway, A. Zunger, W. V. Schoenfeld, and P. M. Petroff, Phys. Rev. B **64**, 165301 (2001).
[17] M. Bayer, G. Ortner, O. Stern, A. Kuther, A. A. Gorbunov, A. Forchel, P. Hawrylak, S. Fafard, K. Hinzer, T. L. Reinecke, S. N. Walck, J. P. Reithmaier, F. Klopf, and F. Schäfer, Phys. Rev. B **65**, 195315 (2002).
[18] J. G. Tischler, A. S. Bracker, D. Gammon, and D. Park, Phys. Rev. B **66**, 081310 (2002).
[19] I. A. Akimov, A. Hundt, T. Flissikowski, and F. Henneberger, Appl. Phys. Lett. **81**, 4730 (2002).
[20] B. Patton, W. Langbein, and U. Woggon, Phys. Rev. B **68**, 125316 (2003).
[21] K. V. Kavokin, Phys. Status Solidi A **195**, 592 (2003).
[22] J. Puls, I. A. Akimov, and F. Henneberger, Phys. Status Solidi B **234**, 304 (2002).
[23] I. A. Akimov, A. Hundt, T. Flissikowski, P. Kratzert, and F. Henneberger, Physica E (Amsterdam) **17**, 31 (2003).
[24] B. Urbaszek, R. J. Warburton, K. Karrai, B. D. Gerardot, P. M. Petroff, and J. M. Garcia, Phys. Rev. Lett. **90**, 247403 (2003).
[25] I. E. Kozin, V. G. Davydov, I. V. Ignatiev, A. V. Kavokin, K. V. Kavokin, G. Malpuech, Hong-Wen Ren, M. Sugisaki, S. Sugou, and Y. Masumoto, Phys. Rev. B **65**, 241312 (2002).
[26] S. Cortez, O. Krebs, S. Laurent, M. Senes, X. Marie, P. Voisin, R. Ferreira, G. Bastard, J.-M. Gérard, and T. Amand, Phys. Rev. Lett. **89**, 207401 (2002).
[27] M. Rabe, M. Lowisch, and F. Henneberger, J. Cryst. Growth **184/185**, 248 (1998).
[28] D. Litvinov, A. Rosenauer, D. Gerthsen, P. Kratzert, M. Rabe, and F. Henneberger, Appl. Phys. Lett. **81**, 640 (2002).
[29] T. Yao, J. Cryst. Growth **72**, 31 (1985).
[30] M. Lowisch, M. Rabe, F. Kreller, and F. Henneberger, Appl. Phys. Lett. **74**, 2489 (1999).
[31] T. Flissikowski, A. Hundt, M. Lowisch, M. Rabe, and F. Henneberger, Phys. Rev. Lett. **86**, 3172 (2001).
[32] I. A. Akimov, T. Flissikowski, A. Hundt, and F. Henneberger, Phys. Status Solidi A **201**, 412 (2004).
[33] A. Lemaitre, A. D. Ashmore, J. J. Finley, D. J. Mowbray, M. S. Skolnick, M. Hopkinson, and T. F. Krauss, Phys. Rev. B **63**, 161309 (2001).
[34] A. V. Koudinov, I. A. Akimov, Yu. G. Kusrayev, and F. Henneberger, Phys. Rev. B **70**, 241305(R) (2004).
[35] O. Z. Karimov, D. Wolverson, J. J. Davies, S. I. Stepanov, T. Ruf, S. V. Ivanov, S. V. Sorokin, C. B. O'Donnell, and K. A. Prior, Phys. Rev. B **62**, 16 582 (2000).